



Water Soluble Iron aminoclay for Catalytic Reduction of Nitrophenol

S. ANBU ANJUGAM VANDARKUZHALI¹, N. RADHA^{1*} and KANNAIYAN PANDIAN^{2*}

¹Department of Chemistry, Seethalakshmi Ramaswami College, Tiruchirappalli - 620 002, India.

²Department of Inorganic Chemistry, University of Madras, Guindy Campus, Chennai - 600 025. India.

(Received: January 15, 2013; Accepted: February 22, 2013)

ABSTRACT

Water soluble iron decorated phyllosilicate is synthesized through one pot sol-gel synthesis by a wet chemical method using NaBH_4 as reducing agent. The as-synthesized nanocomposite is characterized by powder-XRD and TGA techniques. The morphology of the composite is obtained using HRSEM and HRTEM. The prepared nanocomposite is an efficient catalyst for the reduction of nitrophenol.

Key words: Aminoclay, Catalysis, Reduction of nitrophenol.

INTRODUCTION

The uniqueness of noble metal nano particles (MNPs) arises from their size, shape, higher surface to volume ratio with increased percentage of atoms that display superior properties unavailable in conventional macroscopic materials.¹ These have specific properties that differ amazingly from bulk metals and possess promising applications in catalytic and sensor fields²⁻³. Today the need for clean and easily recycled reagents in organic synthesis has meant that solid-supported reagents and scavengers have received more and more attention from organic chemists⁴. Functionalized organic molecules attached covalently to an inorganic surface will yield a new class of inorganic-organic hybrids with unique properties that make these materials a promising class in several applications including catalysis,

sensors, drug delivery and removal of organic pollutants.

Synthetic aminoclay is one of the major class of phyllosilicates is of particular interest owing to their easy synthesis, sorption properties, thermal and mechanical stability and swelling behaviour. Though the chemical modification of the inorganic phyllosilicate frame-works was the aim of several studies, majority of these hybrids has magnesium located inside the lamellar octahedral sites; it could be substituted by nickel,⁴ calcium⁵ and copper.⁶ These clay lamellae can be used to immobilize single biomolecules and proteins such as DNA, Hb, Mb, GOx and these found to exhibit enhanced stability and regenerate without loss of its activity.⁷ Thiol organoclay nanocomposites were used for the adsorption of heavy metal ions⁸ (Hg^{2+} , Pb^{2+} , Cd^{2+}), various anions⁹ (F^- , NO_3^- , PO_4^{3-}), dye adsorption.¹⁰

The selective hydrogenation of aromatic nitro compounds to the corresponding aniline is an industrially important reaction.¹¹ Gold nanoparticle–graphene oxide nanosheets¹³ and silver supported on the CNFs exhibited high catalytic activity in the reduction of nitro compounds.¹³

In this article, we present a simple and facile approach for selective hydrogen transformation of nitroarenes onto the surface of iron NPs in water soluble amino clay sheets. This method not only provides a facile means of controlling the effective concentration of the active Fe NP, but also offers the necessary stability of the resulting nanocomposite for catalytic hydrogen transformation.

EXPERIMENTAL

Materials

3-Aminopropyltrimethoxysilane (APTMS, 99%), Magnesium chloride hexahydrate (98.0%), sodium borohydride (NaBH_4), ferric chloride and nitrophenol were purchased from Sigma-Aldrich (USA). Ethanol (>99.9%) was purchased from Merck. Milli Q water was used for the preparation of aqueous solutions.

Synthesis of aminoclay

Typical synthesis involves drop wise addition of 3-aminopropyltrimethoxysilane (5.85 mmol) to an ethanolic solution of magnesium chloride (3.62 mmol). The white slurry obtained after 5 mins was stirred mechanically overnight. The precipitate was isolated by centrifugation, washed with ethanol (50 mL) and dried at 40 °C.¹⁴

Synthesis of aminoclay stabilized F nanoparticle

The aminoclay was first exfoliated by dispersing 20 mg of clay in 2 mL Milli Q water by sonication for 2 minutes. Metal precursor (1 mM) was added followed by the drop wise addition of NaBH_4 solution (0.1 M).^{14,15} To the resulting transparent suspension, ethanol was added and the freeze dried samples were stored in dark at 5°C.

Reusability

After the reduction reaction, ethanol was added to the solution and the Fe stabilized aminoclay precipitated, was filtered, dried and reused.

RESULTS AND DISCUSSION

The synthesized Fe amino clay nanoparticle was characterized by powder XRD, SEM, EDX and HRTEM techniques and its thermal stability was studied using TGA analysis.

Characterization of aminoclay protected metal nanoparticle

In FTIR spectrum (Figure 2) bands of phyllosilicates are observed in the region 1186 to 1000 cm^{-1} due to Si-O-Si asymmetric stretching. The band near 550 cm^{-1} corresponds to the stretching of Mg-O in the octahedral layer. Bands between 3000 and 2750 cm^{-1} are due to symmetric, asymmetric stretching and deformations of $-\text{CH}_2-$ groups of the 3-aminopropyl groups present in the interlayer space. Bands between 1600 and 1400 cm^{-1} are due to the deformation modes of the amino propyl groups. The reduced peak intensity at 900 cm^{-1} indicates the presence of organic groups in the surface of tetrahedral silicon layers. A very narrow band at 1381 cm^{-1} is due to the formation of the amine carbamate linkage.¹⁶

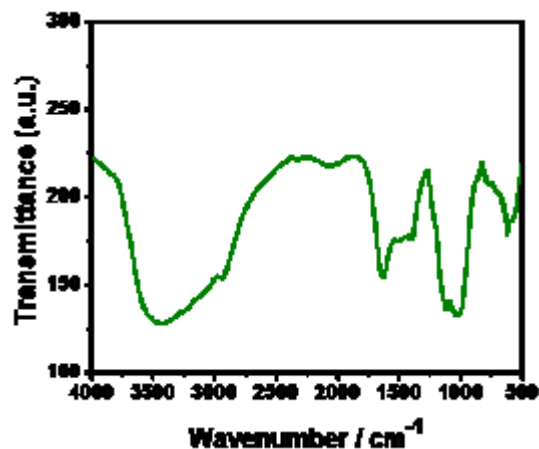


Fig. 2: FT-IR spectra of amino clay Fe nanocomposites

The metallic nature of aminoclay stabilized Fe nanoparticles is confirmed by powder XRD technique (Figure 3). Presence of typical trioctahedral clay is ensured by the signals at 5.3° and 10.4° corresponding to (001) and (002) reflections and at 20°, 35°, and 60° to (020,110),

(130,200) and (060,330) reflections. Aminoclay stabilized iron nanoparticles show four prominent

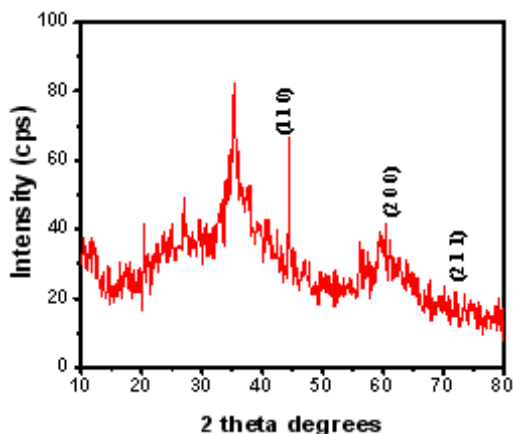


Fig. 3: Powder XRD pattern of Fe aminoclay nanocomposite and corresponding planes.

characteristic peaks at 2θ values of about 48.6, 60.7 and 71.6, representing the (110), (220) and (211) planes of face centered cubic (fcc) structure of Fe (JCPDF No:897194).

Morphological analysis of the materials

Figure 4(a) shows the HRTEM micrographs of highly dispersed amino clay stabilized Fe nanoparticles. Dark spherical spots clearly indicate that Fe nanoparticles are well dispersed throughout the clay matrix. Figure 4(a) shows the metal-loaded hybrid nanocomposites of uniform size and shape and the particle size is around 2-3 nm. Figure 5(b) shows the corresponding selected area electron diffraction (SAED) pattern.

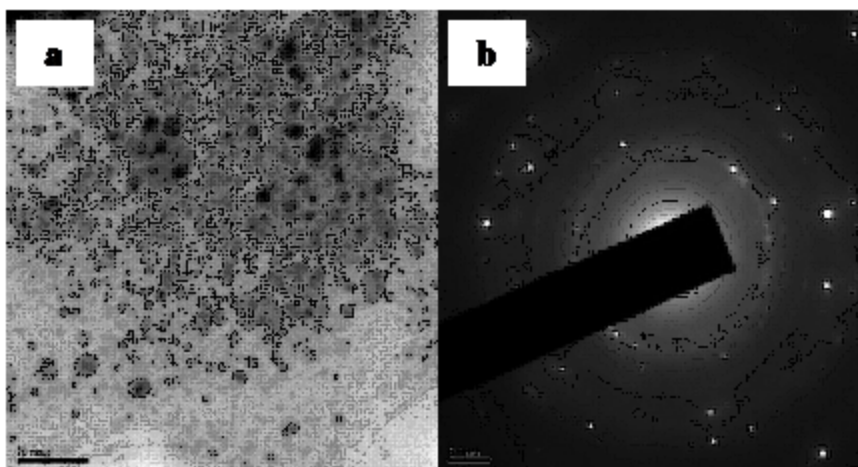


Fig. 4: (a) HRTEM images of highly dispersed aminoclay stabilized Fe nanoparticles. (b) selected area diffraction pattern of aminoclay stabilized Fe nanoparticle in corresponding planes

TGA analysis

Thermal behavior of aminoclay composites are investigated by TGA analysis scanning from 20 – 1000°C (Figure 5). The as prepared phyllosilicate shows four major different weight losses, the curves between 20-140°C and 560-760°C correspond to endothermic peaks while at 140-156°C and 760-810°C exothermic peaks are observed.¹⁷

Catalytic performance of Fe/clay NP in the reduction of 4-Nitrophenol

The catalytic activity of the aminoclay

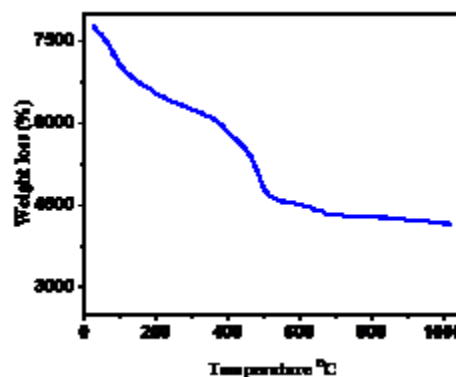
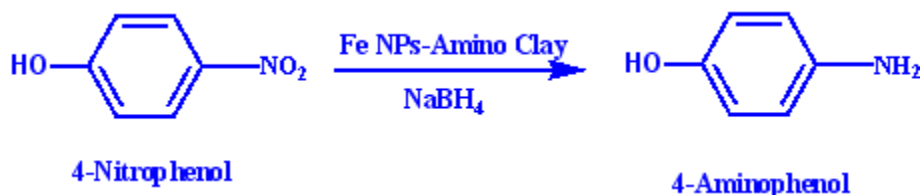


Fig. 5: TGA analysis of Fe aminoclay nanocomposite

nanocomposite was determined using the reduction of 4-nitrophenol by NaBH_4 where the resulting substance 4-aminophenol (Scheme 2) is a commercially important intermediate for the manufacture of analgesic and antipyretic drugs.

Upon the addition of NaBH_4 the absorption peak of 4-nitrophenol (4-Np) undergoes an immediate red-shift from 317 to 400 nm indicating the formation of 4-nitrophenolate ions, evident visibly from the color change of the solution light yellow to yellow green color.



Scheme 1: Reduction of 4-nitrophenol to 4-aminophenol

After the addition of clay nanocomposite the absorption peak at 400nm decreased while the absorption peaks at 300 nm and 230 nm increased attributed to the formation of 4-aminophenol (Amp) as the reaction proceeds Figure 6a. Several isosbestic points indicate the absence of any side products throughout the course of the reaction. In the absence of catalyst, the absorption peak at 400 nm remained unaltered for a long duration, indicating the inability of the strong reducing agent NaBH_4 itself to reduce 4-nitrophenolate ion. Since

the concentration of NaBH_4 is excess throughout the course of the reaction it can be assumed constant.

Therefore, pseudo-first-order kinetics with respect to 4-Np can be used to evaluate the catalytic rate. A good linear correlation was observed between $\ln C_0/C$ vs. reaction time (Figure 6b) and the pseudo-first-order rate constant is estimated from the plot.

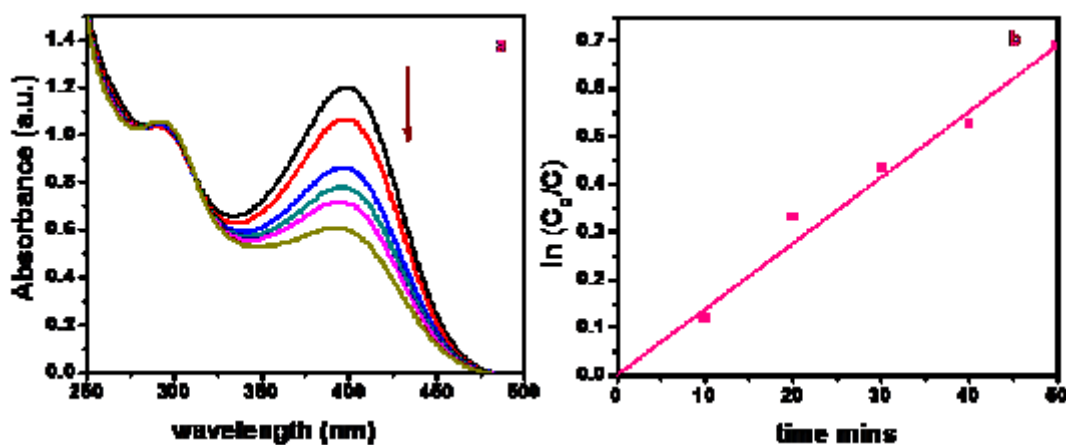


**Fig. 6 (a): UV spectrum of reduction of 4-nitrophenol
(b) Linearized plot of $\ln C_0/C$ showing pseudo first order**

Mechanism of the reduction of 4-Nitrophenol

The reduction of 4-Np compounds is known to proceed *via* the hydroxylamine, followed

by azoxy and azo compounds to its corresponding Amp after the reaction time. To the optimized reaction conditions for the reduction of 4-Np

compound to their corresponding Amp under photolytic conditions proceeds without isolation of the intermediates.

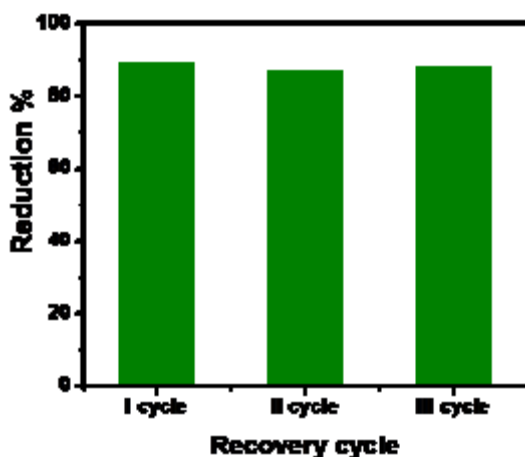


Fig. 7: Recovery cycle of Fe amino clay catalyst

Recycle and reusability of aminoclay protected metal nanoparticles catalyst

The Figure 7 shows the repetitive catalytic degradation of 4-Np during three consecutive cycles. After each catalytic cycle the catalyst was recovered using ethanol and a fresh solution of 4-Np was added before each run. The catalytic efficiency of the catalyst is maintained without any loss in each cycle.

CONCLUSIONS

The catalytic behaviour of the aminoclay stabilized Fe nanoparticle is studied. This nanocomposite is characterized by powder XRD, FTIR, TGA, EDX, HRSEM and HRTEM analyses. This nanocomposite exhibits excellent activity for reduction of nitrophenol. The main advantage of this aminoclay stabilized monohybrids are its ease synthesis, water soluble, cheap source and reusability.

REFERENCES

1. Tagar. Z. A., Sirajuddin, Memon. N., Kalhor. M. S., Kalwar. N. H., Junejo. Y., Hassan. S. S., *Pak. J. Anal. Environ. Chem.*, **13**: 70 (2012).
2. a) Li. J., Liu. C., Liu. Y., *J. Mater. Chem.*, **22**: 8426 (2012).
b) Zheng. Y., Wang. A., *J. Mater. Chem.*, **22**: 16552 (2012).
3. a) Desai, B.; Danks, T. N.; *Tetrahedron Lett.* **42**: 5963 (2001).
b) Danks, T. N.; Desai, B.; *Green Chem.*, **4**: 179 (2002).
c) Desai, B.; Danks, T. N.; Wagner, G.; *Tetrahedron Lett.* **46**: 95 (2005).
4. Fonseca, M. G.; Silva, C. R.; Barone, J. S.; Airoidi, C.; *J. Mater. Chem.*, **10**: 789 (2000).
5. Minet, J.; Abramson, S.; Bresson, B.; Sanchez, C.; Montouillout, V.; Lequeux, N.; *Chem. Mater.* **16**: 3955 (2004).
6. Fonseca, M. G.; Airoidi, C.; *J. Mater. Chem.*, **10**: 1457 (2000).
7. Patil, A. J.; Muthusamy, E.; Mann, S.; *Angew. Chem.*, **116**: 5036 (2004).
8. Li, J.; Zhang, Y.; Cai, W.; Shao, X.; *Talanta*, **84**: 679 (2011).
9. Lee, Y. C.; Kim, E. J.; Shin, H. J.; Choi, M.; Yang, J. W.; *J. Ind. Eng. Chem.* **18**: 871 (2012).
10. Lee, Y. C.; Kim, E. J.; Yang, J. W.; Shin, H. J.; *J. Hazard. Mater.*, **192**: 62 (2011).
11. A.S.Travis, in *The Chemistry of Anilines*, ed. Z. Rappoport, John Wiley & Sons, Ltd, Chichester, England, pp. 715 (2007).
12. Choi, Y.; Bae, H. S.; Seo, E.; Jang, S.; Park, K. H.; Kim, B. S.; *J. Mater. Chem.* **21**: 15431 (2011).
13. Farhad Hatamjafri, *Orient J. Chem.*, **28**(1): (2012).
14. Zhang, P.; Shao, C.; Zhang, Z.; Zhang, M.; Mu, J.; Guo, Z.; Liu, Y.; *Nanoscale*, **3**: 3357 (2011).
15. K. K. R. Datta, M. Eswaramoorthy, C. N. R. Rao, *J. Mater. Chem.*, **17**: 613 (2011).
16. K. K. R. Datta, C. Kulkarni, M. Eswaramoorthy, *Chem. Commun.*, **46**: 616 (2012).
17. R. B. Ferreira, C. R. Silva, H.O. Pastore, *Langmuir*, **24**: 14215 (2008).
18. K. Chabrol, M. Gressier, N. Pebere, M. J. Menu, F. Martin, J. P. Bonino, C. Marichal, J. Brendle, *J. Mater. Chem.*, **20**: 9695 (2012).